American Journal of Physics

PAPERS | OCTOBER 01 2024

Elongation of a ferrofluid droplet near a permanent magnet: A tidal or magnetic energy effect?

Zoe Boekelheide

Am. J. Phys. 92, 752–758 (2024)
https://doi.org/10.1119/5.0207189

Elongation of a ferrofluid droplet near a permanent magnet: A tidal or magnetic energy effect?

Zoe Boekelheide[a)]
Department of Physics, Lafayette College, Easton, Pennsylvania 18042

(Received 6 March 2024; accepted 11 August 2024)

Ferrofluid droplets falling toward a permanent magnet elongate as they approach the magnet. This phenomenon has been proposed as a way to visualize how tidal (nonuniform) forces can cause stretching/elongation of objects, such as the bulging of Earth's oceans under the nonuniform force of the Moon's gravity. In this manuscript, we analyze a ferrofluid in the nonuniform magnetic field of a permanent magnet and compare a simple model for the tidal stretching mechanism with the magnetic energy mechanism, which is known to stretch a ferrofluid droplet even in a uniform magnetic field. Far from the magnet, both mechanisms display power-law behavior as a function of the distance to the magnet z; for the tidal mechanism, the droplet's elongation is proportional to $1/z^8$, while that due to the magnetic energy mechanism is proportional to $1/z^6$. Thus, the elongation of a droplet falling toward a permanent magnet is initially dominated by the magnetic energy effect. The tidal effect overtakes the magnetic energy effect as the droplet approaches the magnet, and at a critical distance, a tidal disruption event occurs. This system can be studied in the laboratory and could be used as an exploratory laboratory for student-designed experimentation.
https://doi.org/10.1119/5.0207189

I. INTRODUCTION

It is commonly known that Earth's ocean tides are related to the Moon's gravity. However, many people (including advanced physics students!) misunderstand the mechanism.[1] Tidal forces in physics refer to nonuniform forces acting on extended bodies; the difference in the force acting on different points on the body leads to stretching or compression. In the case of Earth's ocean tides, the difference in the Moon's $1/r^2$ gravitational force acting on the near and far sides of Earth leads to stretching of Earth's ocean of about half a meter. Tidal effects are ubiquitous in astrophysics; an extreme example is "spaghettification," which refers to the stretching that would occur very near a black hole (usually, as an object is falling into said black hole).[2] How can we demonstrate tidal forces?

Ferrofluids are colloidal suspensions of ferromagnetic particles in a liquid.[*] They are most well-known for the dramatic spiky patterns that occur when a magnetic field is applied perpendicular to a pool of ferrofluid on a surface; the phenomenon is known as normal field instability[3] and an example is shown in Fig. 1(a). Ferrofluid droplets falling toward a permanent magnet elongate in the magnetic field, and it has been reported that the elongation is a demonstration of tidal forces.[2] An example of this elongation from our work is shown in Figs. 1(c)–1(e). The magnetic attractive force due to the permanent magnet's $1/r^3$ field is stronger on the near end of the droplet than the far end, which leads to tidal stretching similar to that of Earth's oceans.

However, free droplets of ferrofluid are known to elongate even in a *uniform* applied magnetic field (see Fig. 1(b)). This happens for the same reason that normal field instability occurs—the elongated shape lowers the droplet's magnetic energy in its own field, a self-energy effect.[†] Which effect dominates when we perform such an experiment? Do ferrofluids falling toward a permanent magnet *demonstrate* tidal forces (i.e., the stretching is truly caused by tidal forces)? Or is it a *visual analogy* (i.e., stretching and tidal forces occur but are not causative)?

In order to understand which mechanism dominates under which circumstance, in this manuscript we analyze ferrofluid droplet elongation in the field of a permanent magnet due to tidal (nonuniform) magnetic forces as well as to the magnetic energy effect which occurs even in a uniform magnetic field.

II. DROPLET AND PERMANENT MAGNET MODEL

A. Permanent magnet

As shown in Fig. 2, assume a permanent magnet with dipole moment $\vec{m}_p$ located at the origin and pointing up. A droplet of ferrofluid is vertically above it, falling down along the magnet's axis, and is instantaneously at position $\vec{z}$. The applied magnetic field $\vec{B}_a$ at $\vec{z}$ along the axis is

$$\vec{B}_a = \mu_0 \vec{H}_a = \frac{\mu_0 m_p}{2\pi z^3}\hat{z}. \tag{1}$$

B. Ferrofluid droplet geometry

Assume the droplet is initially spherical with radius a_0. When stretched, we will approximate it as an ellipsoid (prolate spheroid) with semimajor axis $c > a_0$, semiminor axes $a < a_0$, and constant volume,

[*]Ferrofluids can be purchased from suppliers such as Ferrotec[6] (350 ml for about $100) or in smaller quantities from various vendors on Amazon. They can also be synthesized using fairly straightforward chemistry laboratory techniques.[18]

[†]Interestingly, self-energy effects have been implicated in the gravitational tides of Earth's oceans since the time of Newton,[19] though they are often ignored in simple models. However, in contrast to the situation here, Earth's gravitational self-energy only amplifies the gravitational tidal effect, while magnetic self-energy effects exist even in the absence of magnetic tidal effects.

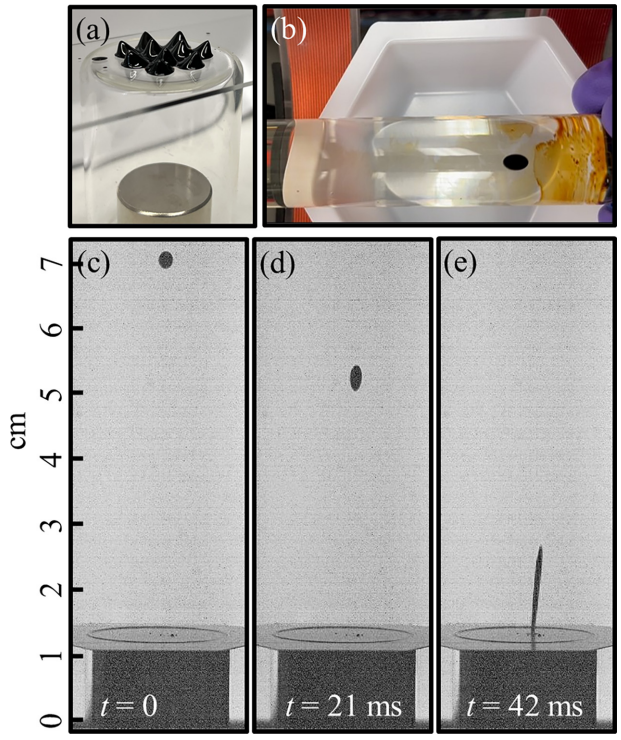

Fig. 1. (a) A ferrofluid exhibiting normal field instability, perhaps the most well-known ferrofluid phenomenon. (b) Elongation of a ferrofluid droplet suspended in corn syrup in a horizontal near-uniform magnetic field generated by Helmholtz coils, captured with a smartphone camera. (c)–(e) Elongation of a ferrofluid droplet as it falls toward a 10.4 A m^2 permanent magnet, captured by a high-speed camera at 1000 fps with 5× shutter speed. (e) is reminiscent of spaghettification.

$$V = \frac{4}{3}\pi a_0^3 = \frac{4}{3}\pi a^2 c. \tag{2}$$

The ellipsoid model is a good approximation for smaller elongations, but experiments have shown more pointed ends when $c/a \gtrsim 2$ (Ref. 4) and close to the magnet, the elongation may be unequal on the near and far sides of the droplet.

The droplet's resistance to stretching comes primarily from the surface energy: $E = \sigma A$, where σ is the surface energy per area and A is the surface area. The surface energy is minimized for a spherical droplet ($c = a_0$) and increases as c varies from a_0 in either direction. Thus, a harmonic approximation to the surface energy is reasonable for small $(c - a_0)$ (Ref. 5). This is equivalent to an ideal spring-like force,

$$F_{\text{spring}} = -kx \quad \text{and} \quad U_{\text{spring}} = \frac{1}{2}kx^2, \tag{3}$$

where x is the elongation of the droplet $2(c - a_0)$. Plotting the surface area of an ellipsoid vs. $(c - a_0)$ can show that a $U \propto (c - a_0)^2$ potential is a good approximation to the surface energy of an ellipsoid for smaller elongations $(c - a_0)/a_0 \lesssim 0.2$.

C. Ferrofluid droplet magnetization

The ferrofluid is an approximately linear magnetic material for low fields, before the ferrofluid approaches saturation. For common commercial ferrofluids, the linear approximation is valid up to around tens of milliTesla.[5–7] In the linear regime, the ferrofluid has intrinsic susceptibility χ and effective susceptibility χ_{eff} such that its magnetization (magnetic moment per unit volume) can be written as

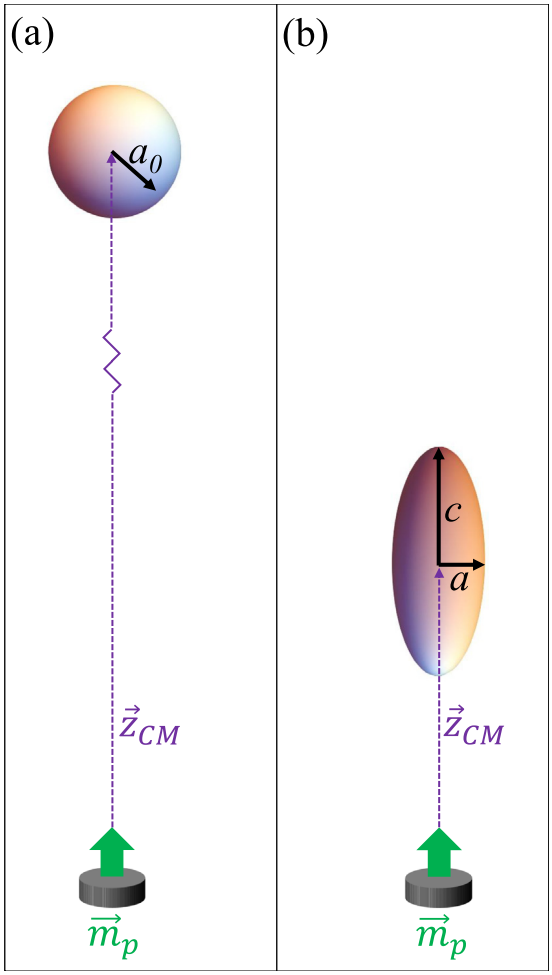

Fig. 2. (a) Initially spherical droplet of ferrofluid with radius a_0, far from a permanent magnet (b) Stretched droplet approximated as a prolate spheroid with semimajor axis $c > a_0$ and semiminor axes $a < a_0$, as it falls toward a permanent magnet.

$$\vec{M} = \chi\vec{H} = \chi_{\text{eff}}\vec{H}_{\text{a}}, \tag{4}$$

and a chunk of ferrofluid with volume v_{f} has moment

$$\vec{m}_{\text{f}} = v_{\text{f}}\vec{M} = v_{\text{f}}\chi_{\text{eff}}\vec{H}_{\text{a}}. \tag{5}$$

Here, $\vec{H}$ is the total $\vec{H}$ field in the droplet: $\vec{H} = \vec{H}_{\text{a}} + \vec{H}_{\text{d}}$, where $\vec{H}_{\text{a}}$ represents the component of $\vec{H}$ from the external permanent magnet while $\vec{H}_{\text{d}}$ is the demagnetizing field due to the ferrofluid's own magnetization. The demagnetizing field can be described by the demagnetizing factor[‡] N_{d}, which depends on the geometry of the object,[8]

$$\vec{H}_{\text{d}} = -N_{\text{d}}\vec{M}. \tag{6}$$

Using Eqs. (6) and (4), it can be shown that

[‡]In general, the demagnetizing field need not be uniform inside an arbitrarily shaped object. Fortunately, a uniformly magnetized ellipsoid is a special case for which the demagnetizing field is uniform and can be described by a single demagnetizing factor.[8]

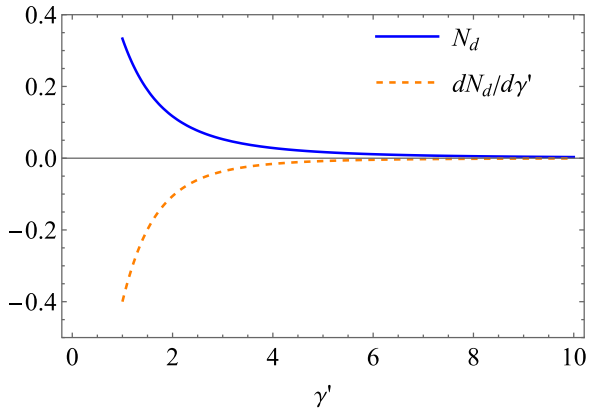

Fig. 3. N_d and $dN_\mathrm{d}/d\gamma'$ as a function of $\gamma' = c/a_0$ from Eq. (9).

$$\chi_\mathrm{eff} = \frac{\chi}{1+\chi N_\mathrm{d}}. \tag{7}$$

The demagnetizing factor N_d for a prolate spheroid[§] is typically written in terms of the aspect ratio $\gamma = c/a$ (Ref. 8). We rewrite it in terms of $\gamma' = c/a_0 = (c/a)^{2/3}$ because in our system a is not a constant.

$$N_\mathrm{d} = \frac{1}{(\gamma^2-1)}\left[\frac{\gamma}{\sqrt{\gamma^2-1}}\ln\left(\gamma+\sqrt{\gamma^2-1}\right)-1\right] \tag{8}$$

$$= \frac{1}{(\gamma'^3-1)}\left[\frac{\gamma'^{3/2}}{\sqrt{\gamma'^3-1}}\ln\left(\gamma'^{3/2}+\sqrt{\gamma'^3-1}\right)-1\right]. \tag{9}$$

$N_\mathrm{d}(\gamma')$ is shown in Fig. 3. It can be seen that, for a spherical droplet ($\gamma' = 1$), $N_\mathrm{d} = 1/3$. As the droplet elongates ($\gamma' \to \infty$), $N_\mathrm{d} \to 0$.

In Secs. III–V, we will study the elongation of a ferrofluid droplet from the magnetic energy and tidal effects as a fraction of a_0, using the "fractional extension" $(c-a_0)/a_0$, or strain, as a metric.

III. MAGNETIC ENERGY IN A UNIFORM MAGNETIC FIELD

There is a magnetic energy effect that causes a ferrofluid droplet to elongate in a magnetic field, even in a uniform magnetic field, as seen in Fig. 1(b). The phenomenon of elongation of ferrofluid droplets due to this magnetic energy effect has been the subject of significant previous and continuing study. In short, for small fields, the fractional extension is proportional to B_a^2 (Ref. 5) (or, $1/z^6$ in a dipole field). Below, we present an analysis that loosely follows that of Bacri and Salin.[4]

The total magnetic energy of a system (assuming only linear magnetic media) is[10]

$$W = \frac{1}{2}\int \vec{B}\cdot\vec{H}\,d\tau, \tag{10}$$

integrated over the entire volume. It can be shown that, when magnetic field sources are fixed, the change in energy upon introducing a piece of linear magnetic material into the system is[3,11]

$$\Delta W = -\frac{1}{2}\int_V \vec{M}\cdot\vec{B}_\mathrm{a}\,d\tau, \tag{11}$$

integrated over the volume of the magnetic material. Thus, the magnetic energy of the material in the presence of the fixed sources (relative to when the material was far away) can be written as[5]

$$U_\mathrm{mag} = -\frac{\mu_0}{2}\int_V \chi_\mathrm{eff} H_\mathrm{a}^2\,d\tau \quad \text{or} \quad -\frac{1}{2\mu_0}\int \chi_\mathrm{eff} B_\mathrm{a}^2\,d\tau. \tag{12}$$

For a uniform applied field and a homogeneous material, the integral is trivial,

$$U_\mathrm{mag} = -\frac{1}{2\mu_0}\chi_\mathrm{eff} B_\mathrm{a}^2 V. \tag{13}$$

Then, plugging Eq. (7) into Eq. (13), the magnetic energy can be written as

$$U_\mathrm{mag} = -\frac{B_\mathrm{a}^2 V}{2\mu_0}\frac{\chi}{1+\chi N_\mathrm{d}}. \tag{14}$$

Since as the droplet elongates, $N_\mathrm{d} \to 0$ (Fig. 3), the magnetic energy (Eq. (14)) of a magnetized droplet is decreased when it is elongated, as expected.

The total energy of the droplet in the presence of a uniform magnetic field is then

$$E_\mathrm{tot} = U_\mathrm{spring} + U_\mathrm{mag} \tag{15}$$

$$= \frac{1}{2}k(2(c-a_0))^2 - \frac{B_\mathrm{a}^2 V}{2\mu_0}\frac{\chi}{1+\chi N_\mathrm{d}}. \tag{16}$$

The energy is minimized when $dE_\mathrm{tot}/dc = 0$

$$\frac{dE_\mathrm{tot}}{dc} = 4k(c-a_0) + \frac{B_\mathrm{a}^2 V}{2\mu_0}\frac{\chi^2}{(1+\chi N_\mathrm{d})^2}\frac{dN_\mathrm{d}}{dc} = 0. \tag{17}$$

Rearranging, the fractional extension due to the magnetic energy effect $((c-a_0)/a_0)_\mathrm{m-e}$ is

$$\left(\frac{c-a_0}{a_0}\right)_\mathrm{m-e} = -\frac{B_\mathrm{a}^2 V}{8\mu_0 k a_0^2}\chi_\mathrm{eff}^2\frac{dN_\mathrm{d}}{d\gamma'}, \tag{18}$$

using the fact that $dN_\mathrm{d}/dc = (dN_\mathrm{d}/d\gamma')(d\gamma'/dc) = (dN_\mathrm{d}/d\gamma')(1/a_0)$.

In the scenario where the applied field is due to an external permanent magnet (Fig. 2), we plug Eq. (1) into Eq. (18) and obtain

$$\left(\frac{c-a_0}{a_0}\right)_\mathrm{m-e} = -\frac{\mu_0 V m_\mathrm{p}^2 \chi_\mathrm{eff}^2}{32\pi^2 k a_0^2 z^6}\frac{dN_\mathrm{d}}{d\gamma'}. \tag{19}$$

A. Approximation: Elongation is small: $((c-a_0)/a_0)_\mathrm{m-e} \ll 1$

For small extensions ($((c-a_0)/a_0)_\mathrm{m-e} \ll 1$, or $\gamma' \sim 1$), the droplet shape is essentially unchanged, so N_d and

[§]A number of different, equivalent expressions have been published. A recent one, written in terms of the eccentricity of the spheroid, can be found in Ref. 9.

$dN_d/d\gamma'$, and therefore χ_{eff} as well, are effectively constant. So, in that regime, by Eq. (18), the fractional extension of the droplet due to the magnetic energy effect $((c-a_0)/a_0)_{m-e}$ is simply $\propto B_a^2$ (Refs. 4, 5, and 12). In the field of a dipole permanent magnet, then, $((c-a_0)/a_0)_{m-e} \propto 1/z^6$.

For large extensions, $N_d(\gamma')$, $dN_d/d\gamma'$, and χ_{eff} cannot be treated as constant, and by Eq. (19), $((c-a_0)/a_0)_{m-e}$ must change more slowly than $1/z^6$. In that case, $((c-a_0)/a_0)_{m-e}$ may be solved for computationally.

IV. MAGNETIC TIDAL FORCE IN A NONUNIFORM MAGNETIC FIELD

Tidal effects arise from force gradients. An excellent resource with a straightforward example analytically deriving the gravitational tidal force on Earth's oceans is Taylor's *Classical Mechanics*.[1] We start with the magnetic force on a chunk of the ferrofluid with moment $\vec{m}_f$,[13]

$$\vec{F} = \vec{m}_f \times (\vec{\nabla} \times \vec{B}_a) + (\vec{m}_f \cdot \vec{\nabla})\vec{B}_a. \tag{20}$$

The first term is zero, and we use Eqs. (1) and (5) to evaluate the second term. Then,

$$\vec{F} = (v_f \chi_{eff} \vec{H}_a \cdot \vec{\nabla})\vec{B}_a \tag{21}$$

$$= \left(v_f \chi_{eff} \frac{m_p}{2\pi z^3}\hat{z} \cdot \vec{\nabla}\right)\left(\frac{\mu_0 m_p}{2\pi z^3}\hat{z}\right) \tag{22}$$

$$= \left(v_f \chi_{eff} \frac{m_p}{2\pi z^3}\right)\left(-3\frac{\mu_0 m_p}{2\pi z^4}\hat{z}\right) \tag{23}$$

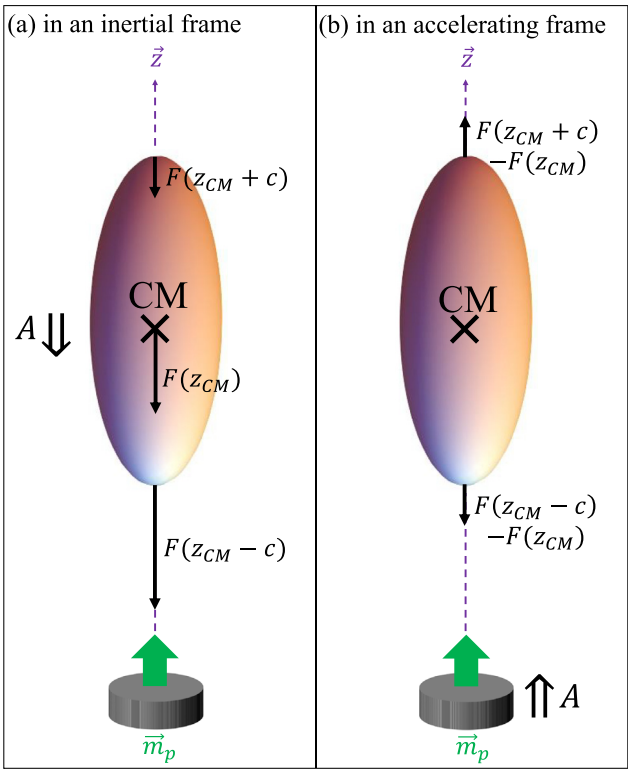

Fig. 4. (a) Forces on parts of the droplet in an inertial reference frame and (b) forces on parts of the droplet in a reference frame that is accelerating with the center of mass of the droplet. Not to scale.

$$= -\left(\frac{3\mu_0 v_f \chi_{eff} m_p^2}{4\pi^2 z^7}\right)\hat{z}. \tag{24}$$

The force on a chunk of ferrofluid in the dipole field of the permanent magnet is strongly nonuniform, as depicted in Fig. 4(a), with a $1/z^7$ dependence on the distance from the permanent magnet. (Note, the $U \propto 1/z^6$, $F \propto 1/z^7$ dependence is a magnetic version of the familiar induced dipole–dipole interaction, like the Van der Waals interaction, the attractive term in the Lennard-Jones potential.[14])

Tidal forces are commonly analyzed within an accelerating reference frame centered on the center of mass (CM) of the object of interest.[1] In this case, we analyze the forces within a frame fixed to the center of the ferrofluid droplet, which is accelerating[**] with $\vec{a} = \vec{F}(\vec{z}_{CM})/m$. In the accelerating reference frame, we add an inertial force $\vec{F}_{inertial} = -m\vec{a}$ to the net force at a given point. Thus, in the accelerating frame, the net force at a given point $\vec{z}$ on the ferrofluid is given by the difference in forces between that point and $\vec{z}_{CM}$, in the inertial frame, as shown in Fig. 4(b).

The tidal force is the force difference,

$$\vec{F}_{tidal} = \Delta\vec{F} = \vec{F}(\vec{z}) - \vec{F}(\vec{z}_{CM}), \tag{25}$$

which, for points along the axis of $\vec{m}_p$ above the permanent magnet, becomes

$$\vec{F}_{tidal} = -\frac{3\mu_0 v_f \chi_{eff} m_p^2}{4\pi^2}\left(\frac{1}{z^7} - \frac{1}{z_{CM}^7}\right)\hat{z}. \tag{26}$$

Applying the ideal spring-force model to points on the near and far ends of the droplet, in equilibrium the stretching tidal force must be balanced by the spring force,

$$-\frac{3\mu_0 v_f \chi_{eff} m_p^2}{4\pi^2}\left(\frac{1}{z^7} - \frac{1}{z_{CM}^7}\right) = k_f x \tag{27}$$

or,

$$\mp\frac{3\mu_0 v_f \chi_{eff} m_p^2}{4\pi^2}\left(\frac{1}{(z_{CM} \pm c)^7} - \frac{1}{z_{CM}^7}\right) = 2k_f(c-a_0). \tag{28}$$

Here, $z = z_{CM} \pm c$ refer to the far and near sides of the droplet, respectively, and the $\mp$ in front of the expression ensures that the magnitude of the force is positive. The extension of the droplet $x = 2(c-a_0)$, and k_f is the spring constant corresponding to displacement of a chunk v_f. Two factors make it challenging to solve this equation for c, or the fractional extension of the droplet $(c-a_0)/a_0$, on the near and far sides of the droplet: First, solutions to high order polynomial equations are messy, and second, χ_{eff} actually depends on c as we saw in Sec. III. However, there are two different conditions that allow us to make simplifying approximations to

[**]Note that here we are ignoring an additional uniform acceleration $\vec{g}$ due to gravity, assuming we pursue this demonstration on Earth in the configuration shown in Fig. 2. Gravitational acceleration has no effect except to make the droplet fall faster; it could, therefore, change the dynamics of the system (e.g., does the droplet have time to stretch to reach equilibrium?) but such dynamics are beyond the scope of this manuscript.

gain analytical insight into this system. The first is when $z \gg c$, and the second is when $(c - a_0)/a_0 \ll 1$. When these approximations are not valid, we can numerically calculate the solution.

A. Approximation: z is large: $z \gg c$

When the droplet is far from the magnet ($z \gg c$), the tidal force varies approximately linearly across the droplet and can be approximated as[15]

$$F_{\text{tidal}} = \Delta F = \left(\frac{dF}{dz}\right)\Delta z = \pm\left(\frac{21\mu_0 v_f \chi_{\text{eff}} m_p^2}{4\pi^2 z^8}\right)\Delta z \tag{29}$$

for small deviations Δz around a given z, and can be assumed to be equal and opposite on the near and far sides of the droplet. So, because the magnetic force goes like $1/z^7$, the tidal force (proportional to the force gradient) goes like $1/z^8$—just as how, for the gravitational force $\propto 1/r^2$, gravitational tidal forces go like $1/r^3$ (Refs. 1 and 15).

Then, balancing the tidal force with the spring force,

$$F_{\text{tidal}} = \left(\frac{21\mu_0 \chi_{\text{eff}} v_f m_p^2}{4\pi^2 z^8}\right)\Delta z = k_f x \tag{30}$$

$$= \left(\frac{21\mu_0 \chi_{\text{eff}} v_f m_p^2}{4\pi^2 z^8}\right) c = 2k_f(c - a_0). \tag{31}$$

We can then write the fractional extension of the droplet as

$$\left(\frac{c - a_0}{a_0}\right)_{\text{tidal}} = \left(1 - \frac{1}{2}\frac{21\mu_0 \chi_{\text{eff}} v_f m_p^2}{4\pi^2 k_f z^8}\right)^{-1} - 1. \tag{32}$$

Because χ_{eff} depends on c, this is not actually a solution until we make a second approximation.

B. Approximation: Elongation is small: $((c - a_0)/a_0)_{\text{tidal}} \ll 1$

When $z \gg c$ and also the fractional extension is small, $((c - a_0)/a_0)_{\text{tidal}} \ll 1$, the $1/z^8$ term in Eq. (32) must be small, so the binomial approximation can be used. In addition, when the fractional extension is small, $((c - a_0)/a_0)_{\text{tidal}} \ll 1$, the droplet shape is basically unchanged and so χ_{eff} is effectively constant as in Sec. III A. Then, Eq. (32) can be approximated as

$$\left(\frac{c - a_0}{a_0}\right)_{\text{tidal}} = \frac{21\mu_0 \chi_{\text{eff}} v_f m_p^2}{8\pi^2 k_f z^8}. \tag{33}$$

So, the fractional extension of the droplet due to the tidal effect $((c - a_0)/a_0)_{\text{tidal}} \propto 1/z^8$ for small $((c - a_0)/a_0)_{\text{tidal}}$ and large z.

C. Critical z

From Eq. (32), there seems to be a critical z for which $((c - a_0)/a_0)_{\text{tidal}} \to \infty$, and we can obtain a rough estimate for the critical distance from the permanent magnet,

$$z_{\text{crit}} \approx \left(\frac{21\mu_0 \chi_{\text{eff}} v_f m_p^2}{8\pi^2 k_f}\right)^{1/8}. \tag{34}$$

In the exact equation (Eq. (28)), the critical distance corresponds to the distance z_{CM} below which there is no positive, real solution for c on the near side of the droplet.

Physically, at the critical distance, the tidal force on the near side of the droplet exceeds the possible restoring spring force, so the forces on the near end of the droplet are not in equilibrium. The droplet stretches rapidly until the near end is pulled into the magnet in a tidal disruption event. This means that, for large extensions, the fractional extension increases *more rapidly* than $1/z^8$.

The critical distance z_{crit} is analogous to the Roche limit in astrophysical tidal systems. The Roche limit is the minimum orbital radius at which an orbiting body can remain intact; for orbital radii below the Roche limit, an orbiting body is pulled apart by tidal forces.[15]

V. COMPARING THE TIDAL AND MAGNETIC ENERGY EFFECTS

When z is large and the extension of the droplet is small, both tidal and magnetic energy effects lead to fractional extensions of the ferrofluid droplet that obey simple power

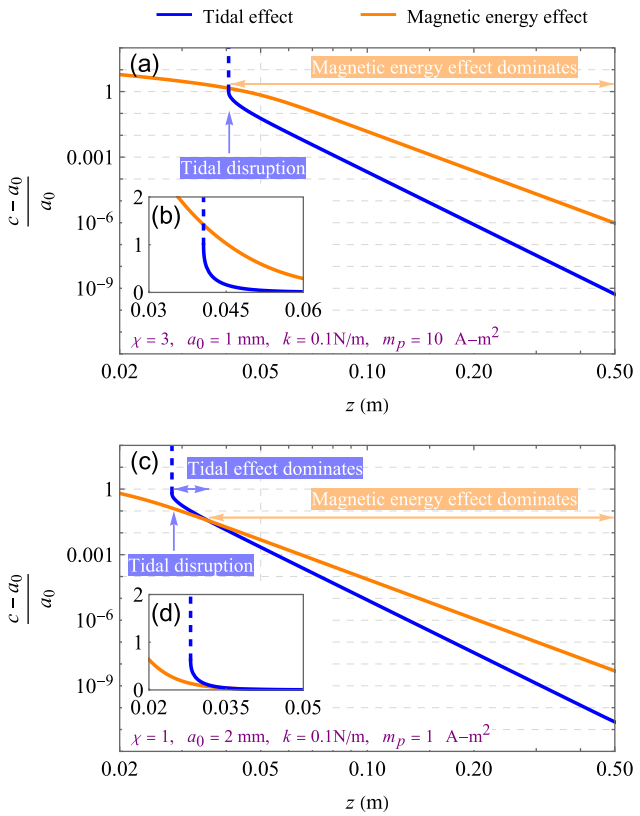

Fig. 5. Numerical calculation of the fractional extension of the ferrofluid droplet due to the tidal effect and the magnetic energy effect for two sets of parameters. (a) Log scale and (b) linear scale for a calculation using $\chi = 3$, $a_0 = 0.001$ m, $k = 0.1$ N/m, and $m_p = 10\,\text{A}\,\text{m}^2$. (c) Log scale and (d) linear scale for a calculation using $\chi = 1$, $a_0 = 0.002$ m, $k = 0.1$ N/m, and $m_p = 1\,\text{A}\,\text{m}^2$. The orange solid lines are calculated using Eq. (19) and the blue solid lines are calculated using the average of the solutions to Eq. (28) for the near and far sides of the droplet. The dashed blue lines are not a solution to the mathematical equilibrium equation but represent the expected physical response to nonequilibrium conditions at the critical distance.

laws. In that regime, we expect the magnetic energy effect ($\propto 1/z^6$) to dominate the tidal effect ($\propto 1/z^8$).

When these approximations are not valid, we can numerically calculate the fractional extension $(c-a_0)/a_0$ due to the tidal effect (Eq. (28)) and due to the magnetic energy effect (Eq. (19)). To compare the tidal model (which analyzes a chunk of ferrofluid with volume v_f and spring constant k_f) with the magnetic energy model (which analyzes the entire droplet with volume V and spring constant k), we make the reasonable assumption that $v_f/k_f \approx V/k$.

Such a calculation is shown in Fig. 5 for two sets of representative parameters. The calculations are shown on log–log axes in Figs. 5(a) and 5(c) so that the power-law behavior is evident at large z, with the magnetic energy effect dominating. Deviations from the power-law behavior are evident at smaller z. As z decreases, the tidal effect overtakes the magnetic energy effect, and at a critical distance from the magnet, the droplet rapidly elongates until the near end is sucked onto the magnet in a tidal disruption event, represented by the dashed blue lines in Fig. 5.

The exact point of crossover between the magnetic energy regime and the tidal regime depends on the details of the ferrofluid and the permanent magnet. For the parameters used in Figs. 5(a) and 5(b) (large magnet, large χ, and small droplet), the magnetic energy effect clearly dominates for almost the entire range of z—essentially until the critical distance at which the tidal disruption event occurs. However, for the parameters used in Figs. 5(c) and 5(d) (smaller magnet, smaller χ, and larger droplet), while the magnetic energy effect dominates at large z, the tidal effect begins to dominate earlier, and in fact dominates for most of the range of z at which droplet extension would be visible by eye. The insets shown in Figs. 5(b) and 5(d) show the same numerical calculations on a linear scale, more relevant to what an experimenter would observe by eye or with a camera.

To understand where this crossover occurs more systematically, we can find the value of z for which $((c-a_0)/a_0)_{\text{tidal}} = ((c-a_0)/a_0)_{\text{m-e}}$. Using the simple power-law relations of Eqs. (33) and (19), that value for z is given by

$$z_{\text{crossover}} \approx \sqrt{\frac{84}{\chi_{\text{eff}}\left|\frac{dN_d}{d\gamma'}\right|}}\,a_0. \tag{35}$$

For the representative values used in Figs. 5(a) and 5(b), then, the two effects should be approximately equal when $z \approx 12$ mm, while for those used in Figs. 5(c) and 5(d), the two effects should be approximately equal when $z \approx 33$ mm. In the numerical calculation, the crossovers occur at somewhat higher values of z because of the deviations from the power-law behavior.

Finally, we can return to the question: Which mechanism dominates the elongation of the ferrofluid droplet—the magnetic energy effect or the tidal effect? Clearly, the magnetic energy effect must dominate at large z. At small z, we expect the tidal effect to dominate at least momentarily at the critical z at which there is a tidal disruption event. Is the tidal effect significant outside of that critical event? To answer this, we can compare z_{crit} from Eq. (34) and $z_{\text{crossover}}$ from Eq. (35). If $z_{\text{crossover}} > z_{\text{crit}}$ then the tidal effect is significant for a range of z before the tidal disruption event occurs, like in Figs. 5(c) and 5(d). If $z_{\text{crossover}} < z_{\text{crit}}$ then the tidal effect is only significant momentarily at the critical z, like in Figs. 5(a) and 5(b).

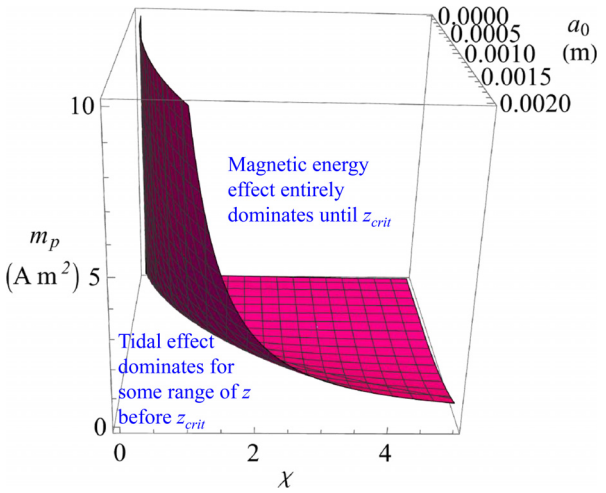

Fig. 6. Contour of $z_{\text{crit}} = z_{\text{crossover}}$ for a range of a_0, m_p, and χ with $k = 0.1$ N/m. For sets of parameters above the contour, the magnetic energy mechanism dominates the entire time up until z_{crit}. For sets of parameters below the contour, the tidal effect is significant for a range of z.

Figure 6 maps $z_{\text{crit}} = z_{\text{crossover}}$ for a range of a_0, m_p, and χ values. For sets of parameters above the surface, the magnetic energy effect dominates the entire time (up until z_{crit}), whereas for sets of parameters below the surface, the tidal effect dominates for some range of z before z_{crit}. The magnetic energy effect dominates when χ is large since two factors of χ appear in Eq. (19) and only one in Eq. (33). The tidal effect dominates for larger droplets since there is a larger force difference between the near and far sides of the droplet. Tidal forces are also more significant for smaller permanent magnet moments m_p because, at a distance z to achieve a given magnetic field, the field gradient is larger for the smaller magnetic moment magnet than a larger one.

VI. USE IN EDUCATIONAL SETTINGS

These models can be understood almost entirely using physics textbooks at the level of the advanced undergraduate, many of which are classic texts that physics majors will be familiar with from coursework.[1,13–15] Details of the magnetic energy are accessible to advanced undergraduates,[8] though they may not yet have familiarity with the details unless they have studied magnetism.

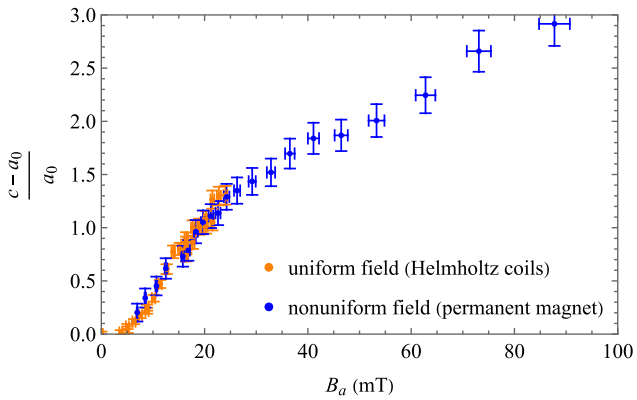

Fig. 7. Fractional extension of ferrofluid droplets measured with a high-speed camera, dropped through a nearly uniform field (from Helmholtz coils) compared to a nonuniform field (from a permanent magnet).

Aspects of these models can be tested experimentally by students in a variety of creative ways using affordable and easily accessible equipment such as permanent magnets to create nonuniform fields, electromagnets to create near-uniform fields, and commercially available ferrofluid. A high-speed camera (≥ 1000 frames per second) is useful for capturing falling droplets, if available (Figs. 1(c)–1(e)). However, static effects can be tested on ferrofluid droplets in water or corn syrup with a simple smartphone camera (Fig. 1(b)).

Figure 7 shows one possible such dataset: the measured fractional extension of $\sim 10\,\mu$l ferrofluid droplets (nominal $\chi = 2.64$ (Ref. 6)) measured with a high-speed camera as a function of the magnetic field in two scenarios: falling through a nearly uniform magnetic field generated by Helmholtz coils and falling through a nonuniform magnetic field toward a permanent magnet ($1''$ length $\times$ $7/8''$ diameter, NdFeB, Grade N42 (Ref. 16) with moment $10.4\,\mathrm{A\,m^2}$). To compare droplets, a consistent droplet size is recommended, so a micropipette is useful. The images in Figs. 1(c)–1(e) are from this experiment.

In this case, the fractional extension in the two scenarios is the same, within the uncertainty, in the field range in which the data overlap, so the data support that the primary mechanism for droplet elongation as it approaches this magnet is the magnetic energy effect rather than tidal forces, as expected for this set of experimental parameters from Fig. 6. The B_a^2 behavior can be observed at low fields and elongations, with deviation from that behavior at larger fields.

One significant source of error in the measurement of falling droplets is the time needed for the droplet to deform—a few milliseconds delay can be significant for droplets measured at ≥ 1000 frames per second. This error is more significant when using smaller permanent magnets (0.1–$1\,\mathrm{A\,m^2}$) because measurable deformations occur near the magnet where the field gradient is very high and the droplet experiences a rapidly increasing field.

VII. CONCLUSION

The American Association of Physics Teachers (AAPT) advises that students in undergraduate physics laboratories should be involved in constructing knowledge, including posing scientific questions themselves and designing experiments to answer those questions.[17] We suggest the topic of elongation of ferrofluid droplets in an applied magnetic field as an open-ended laboratory project in which students can pose their own scientific questions and then design their own experiments. In doing so, they could test the models or parts of the models delineated here, which they can understand using their advanced undergraduate physics knowledge. They might find it particularly interesting given that it is a topic that has been popularized by a video with millions of views.[2] In the Advanced Physics Laboratory course at our small liberal arts college, students designed and implemented experiments to: test the elongation of ferrofluid droplets in a uniform field (Helmholtz coils) to verify the B_a^2 dependence at low fields; measure χ of the ferrofluid; and identify the oscillation modes of ferrofluid droplets exposed to slowly vibrating permanent magnets.

ACKNOWLEDGMENTS

The author thanks Oscar Jopp, Vanessa Haraya Dela Paz Maca, Kevin Manogue, Luke Martin, John C. Santos III, and Henry Steinthal who provided valuable insights at an early stage of the project. The author also thanks Jeffrey Helm for use of a high-speed camera, Aidan Wensel for collaboration on ferrofluid photos, and Jackson Miller and Andrew Dougherty for useful discussion.

AUTHOR DECLARATIONS

Conflict of Interest

The author has no conflicts to disclose.

[a]Electronic mail: boekelhz@lafayette.edu, ORCID: 0000-0003-3212-3171.

[1]J. R. Taylor, *Classical Mechanics* (University Science Books, 2005), pp. 327–336.

[2]D. Cowern, see https://www.youtube.com/watch?v=04v4qWVtdPs for "Slow Motion Science! Ferrofluid Dropping on Magnet" (2017).

[3]R. E. Rosensweig, *Ferrohydrodynamics* (Dover Publications, 1997), pp. 95–98.

[4]J. C. Bacri and D. Salin, "Instability of ferrofluid magnetic drops under magnetic field," J. Phys. **43**, L649 (1982).

[5]C. Wischnewski and J. Kierfeld, "Spheroidal and conical shapes of ferrofluid-filled capsules in magnetic fields," Phys. Rev. Fluids **3**, 043603 (2018).

[6]Ferrotec, see https://ferrofluid.ferrotec.com/products/ferrofluid-educational-fluid/efh/efh1/ for "EFH1 Specifications and Physical Properties" (accessed August 22, 2023).

[7]Z. Boekelheide and C. L. Dennis, "Artifacts in magnetic measurements of fluid samples," AIP Adv. **6**, 085201 (2016).

[8]B. D. Cullity and C. D. Graham, *Introduction to Magnetic Materials*, 2nd ed. (IEEE Press, 2009), pp. 53–54 and 65.

[9]A. Garg, J. B. Ketterson, and J. Lim, "A novel method of images for solving Laplace's equation and deriving demagnetization factors for spheroidal bodies," Am. J. Phys. **90**(7), 520–528 (2022).

[10]J. D. Jackson, *Classical Electrodynamics*, 3rd ed. (John Wiley & Sons, Inc., 1999), p. 213.

[11]J. A. Stratton, *Electromagnetic Theory* (IEEE Press, 2007), p. 128.

[12]For example, when $((c-a_0)/a_0)_{\mathrm{m-e}} = 0.01$ (a reasonable upper limit for the $((c-a_0)/a_0)_{\mathrm{m-e}} \ll 1$ regime), N_d and $|dN_\mathrm{d}/d\gamma'|$ are each only reduced by about 1%–1.5% from their value at $((c-a_0)/a_0)_{\mathrm{m-e}} = 0$. This is a very small effect on $((c-a_0)/a_0)_{\mathrm{m-e}}$ compared to the $1/z^6$ term.

[13]D. J. Griffiths, *Introduction to Electrodynamics*, 5th ed. (Cambridge U. P., 2024), pp. 254, 271, and 287.

[14]C. Kittel, *Introduction to Solid State Physics*, 8th ed. (John Wiley and Sons, Inc., 2005), pp. 53–56.

[15]B. W. Carroll and D. A. Ostlie, *An Introduction to Modern Astrophysics*, 2nd ed. (Cambridge U. P., 2017), pp. 719–724.

[16]K. J. Magnetics, see https://www.kjmagnetics.com/blog.asp?p=dipole for "Magnetic Dipole Moment" (accessed February 27, 2024).

[17]J. Kozminski *et al.*, in AAPT Recommendations for the Undergraduate Physics Laboratory Curriculum, 2014. https://www.aapt.org/Resources/upload/LabGuidlinesDocument_EBendorsed_nov10.pdf.

[18]P. Berger, N. B. Adelman, K. J. Beckman, D. J. Campbell, A. B. Ellis, and G. C. Lisensky, "Preparation and properties of an aqueous ferrofluid," J. Chem. Educ. **76**(7), 943 (1999).

[19]T. Norsen, M. Dreese, and C. West, "The gravitational self-interaction of the Earth's tidal bulge," Am. J. Phys. **85**, 9 (2017).